Compact Beam-Steerable Lens Antenna for 60-GHz Wireless Communications

Jorge R. Costa, *Member, IEEE*, Eduardo B. Lima, and Carlos A. Fernandes, *Senior Member, IEEE*

Pls update to: "Senior Member"

***Abstract*—This paper presents a new concept of steerable beam antenna composed by a dielectric lens which pivots in front of a single stationary moderate gain feed. The lens not only allows steering mechanically the beam in elevation and full azimuth, but further increases the gain up to 21 dBi. The solution is broadband, including the entire international unlicensed spectrum from 57 GHz to 66 GHz. A fabricated prototype shows the possibility of tilting the beam from -45° to $+45^\circ$ for all azimuths with gain scan loss below 1.1 dB and radiation efficiency above 95%. The arrangement is very simple, it does not require rotary joints, it is low cost and compact, lens plus feed volume being of the order of $3 \times 3 \times 3$ cm^3 with lens weight less than 10 g.**

***Index Terms*—Compact lens antennas, 60-GHz wireless communication, low-cost, mechanical beam-steering.**

I. Introduction

RECENTLY a new emerging wireless communication standard is being developed to use the world unlicensed spectrum from 57 GHz to 66 GHz [1], [2]. Those frequencies can support very high bit-rate transmission; however, atmospheric impairments limit radio link range to a few hundred meters. Therefore, a new wireless high definition entertaining network (WirelessHD) is being developed for this band to provide indoor communication between terminals requiring high bit-rates, like connecting the Blue Ray recorder, a portable high-definition (HD) game console or a camcorder to a full HD flat screen. To improve the link budget and ensure acceptable system performance and range, antennas with gains greater than 14 dBi or even 20 dBi are required. As a result of the inherent narrow beam, steerable beam capability is envisaged to automatically point the main beam to the direction of a transmitting device or even to follow a moving portable device. Other strategies were explored in the past for similar requirements resorting to constant flux shaped beams without restricting the mobility [3]–[5], but the new emerging standard is pointing in the direction of beam-steered antenna solutions. Antenna compactness and low-cost are of course desirable features for WirelessHD applications.

Manuscript received June 25, 2008; revised September 27, 2008. First published August 04, 2009; current version published October 07, 2009.

J. R. Costa is with the Instituto de Telecomunicações, IST, 1049-001 Lisboa, Portugal, and also with the Instituto Superior de Ciências do Trabalho e da Empresa, Departamento de Ciências e Tecnologias da Informação, 1649-026 Lisboa, Portugal (e-mail: Jorge.Costa@lx.it.pt).

E. B. Lima and C. A. Fernandes are with the Instituto de Telecomunicações, IST, 1049-001 Lisboa, Portugal.

Color versions of one or more of the figures in this paper are available online at http://ieeexplore.ieee.org.

Digital Object Identifier 10.1109/TAP.2009.2029288

Beam-steering can be performed mechanically by moving all or some part of the antenna [6]–[8], electrically by using phased array antennas or switched multiple feed antennas [9]–[11], or by combining the two techniques. Electrical steering has the advantage of being faster than mechanical solutions however, at millimeter waves, efficiency, phase stability and cost are quite critical issues for phased arrays, especially when using MMIC technology to reach mass applications. These issues are being tackled, but as an example, the Ka band antenna implementation reported in [9], using RF MEMS as time delay units for the phasing circuit of a 1×8 element array, presents efficiency of the order of 25% yielding 10 dBi gain. Scanning is in one plane only. Other approach combining a constrained lens with a dome lens is reported in [12], but again the obtained gain is of the order of 10 dBi for a 10λ diameter radome.

Imaginative solutions are reported for mechanical steering that could be appropriate for low-cost implementation at millimeter waves. In [7] a reflectarray is presented that is formed by $1 \times$ N array of rotating circular disks shorted at the periphery. For circular polarized wave incidence, the direction of the reflected beam is controlled by the difference of rotating speeds of the disks. In [13], a solution is presented, based on cylinder metal grating that spins close to two dielectric waveguides perturbing the propagation of the evanescent wave along the waveguide thus controlling its diffraction. The scanning angle is however dependent on frequency and scanning is in one plane. In [8] a similar concept is presented using a diff[illegible] with the same inconvenient.

replace by "tracking"

This paper adopts a mechanical steering approach that does not suffer from previous limitations, intended for the antenna that is mounted for instance in the HD screen, as a low-cost and efficient compromise solution for slower racking situations that are most common when pointing in the direction of a HD equipment in the room that is still or is held by a person. Indicative specifications taken here for proof of concept are: > 20 dBi gain steerable-beam, $> 40^\circ$ elevation beam tilt with gain scan loss < 2 dB, full azimuth scan, and radiation efficiency $> 95\%$; furthermore, the antenna is required to be compact, simple and adequate for low-cost mass production.

The proposed antenna solution consists of an axial symmetric dielectric lens that pivots with a simple two axis movement in front of a moderate directivity stationary feed. The lens main function is to tilt the beam with respect to the fixed feed axis, within a wide conic angular sector. The lens is used also to collimate the beam in order to push the gain up to more than 20 dBi. These two functions require appropriate shaping of the top and bottom lens surfaces, which is the key factor for the usefulness of the proposed solution. The resulting antenna assembly is simple, it is reasonably small with wide-angle scanning; the lens

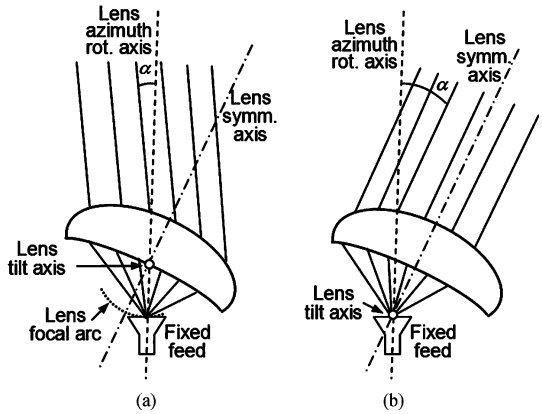

Fig. 1. Two axis pivoting lens placed in front of a fixed feed for beam-steering. (a) Lens tilt axis centered with respect to its focal arc. (b) Tilt axis passing through lens focal point.

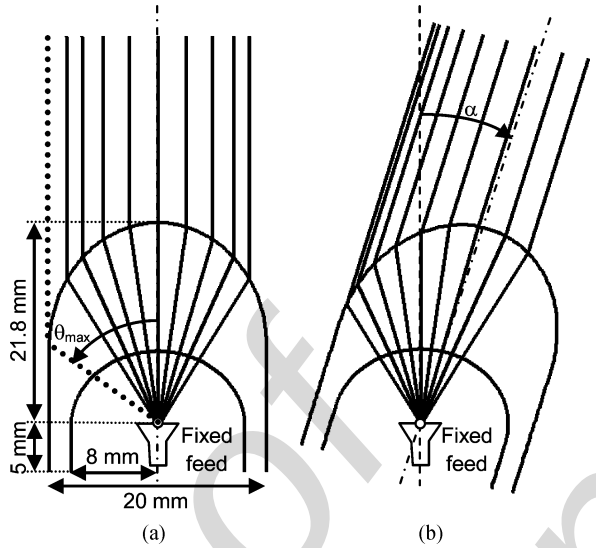

Fig. 2. Ray tracing in polyethylene elliptical lens with spherical air cavity. (a) zero-tilt case. (b) $\alpha = 15^\circ$ lens-tilt.

can be fabricated using a molding process. The feed is intentionally chosen to be stationary, in order to dispense expensive and fault prone millimeter-wave rotary joints. All these characteristics favor the objective of a very low-cost solution.

This is opposed to the classical concept of scanning lenses where the lens is stationary and a cluster of feeds is distributed over the lens focal arc [14]. Any of these or other reported mechanical steering antennas are more complex, larger and more costly at millimeter waves than our proposed solution.

This paper is organized as follows. The antenna concept is presented in Section II. The design and performance of a lens solution with a single refraction surface are presented in Section III. Section IV presents an improved lens solution with two refraction surfaces. In both cases, numerical and experimental results are given and discussed. Conclusions are finally drawn in Section V.

II. Concept Description

The challenge here is to comply with the previously referred specifications using just one pivoting element in front of the fixed feed, to keep with a very simple and reliable structure.

One obvious possibility would be to place a conventional scanning lens in front of the stationary feed and tilt the lens in such a way that its focal arc always contained the feed phase center [Fig. 1(a)]. However, it can be shown that the resulting maximum scanning angle α is very limited in this case.

The approach in this paper is to tilt a collimated beam lens about its central focal point [Fig. 1(b)]; this makes all the difference. In this way the lens does not need to comply with a scanning beam condition, which thus leaves more degrees of freedom for lens profile optimization. Being a collimated beam lens with centered feeding, the output rays always emerge parallel to the lens symmetry axis, making the α beam tilt angle to be the same as the lens tilt angle. The azimuth beam scanning is obtained by simultaneous rotation of the lens about the feed axis.

The issues to consider when designing the collimated beam lens are the maximum achievable beam tilt angle, the maximum gain and the minimum gain scan loss. These characteristics are determined by the lens profile of course, but they are in part limited by reflections at the dielectric interfaces and by feed illumination spillover as lens tilt increases. An appropriate feed must be designed for proper lens illumination.

Two lens geometries are presented: one is based on a single refraction surface configuration that is used for easy explanation of the concept and its limitations; the second lens, based on double-refraction lens, is optimized to tackle those limitations and present improved performance.

III. Solution With Single Refraction Surface

A. Lens Configuration

The elliptical lenses are common solutions to obtain collimated beams [15]–[17]: rays departing from the feed immersed in the dielectric at the ellipse focal point emerge from the lens surface parallel to the lens axis. For low loss dielectric materials, the lens antenna gain is mostly determined by its aperture size.

In order to be able to tilt the lens without tilting the feed, it must be detached from the lens. Using the same approach that the authors adopted for a LEO satellite lens application [18], a spherical air dome can be opened at the base of the lens, centered with the feed phase centre (Fig. 2). The spherical cavity does not introduce major modifications to the feed's illumination of the lens elliptical surface since the lens inner interface does not produce any refraction. In this way the lens can tilt and steer the beam in elevation, while the feed remains stationary at the focal point.

Fig. 2 shows a ray tracing in an extended hemi-elliptical lens with inner air cavity for two lens tilts. It illustrates that the output rays always emerge parallel to the lens axis, and so the beam tilt is the same as the lens tilt. For any lens tilt, the lens can rotate about the feed axis to produce an azimuth beam scan.

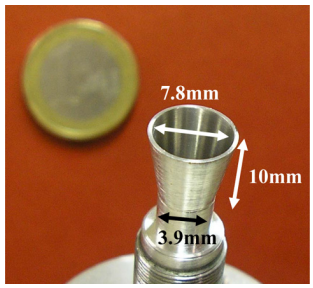

Fig. 3. Photograph of the manufactured circular horn feed.

It is noted that the subtended angle of the feed radiation θ must be restricted in order to avoid that peripheral rays exceed the lens collimating region. Based upon Geometrical Optics (GO), the collimating region corresponds to

$$\theta < \theta_{\max} = \operatorname{acos}\left(\frac{1}{\sqrt{\varepsilon_r}}\right) \quad (1)$$

where ε_r is the lens material permittivity and θ is the angle between a ray path departing from the feed and the lens axis; $\theta_{\max}$ value corresponds to the first ray that hits the external cylinder wall of the lens. For larger angles, rays are refracted away from the main beam direction, contributing to side lobes and to lowering gain. For a given feed, the impact of this effect is higher as the lens tilt increases, originating gain scan loss.

B. Circular Horn Feed

The feed must be designed such that its radiation is negligible at $\theta_{\max}$ for the maximum lens tilt, which points to a moderate directivity feed radiation pattern. A compromise is also needed with the feed aperture size to fit into the spherical air cavity at the focal point and further allow space for lens tilting without being impaired by the feed. Calculations showed that feed directivity in the range 13–14 dBi is adequate for the envisaged lenses.

As for polarization, considering that the equipment at the other end of the link is potentially portable, circular polarization (CP) was preferred here over linear polarization. Anyway, the concept remains valid and feasible for linear polarization.

Given the above, a conical horn antenna is a natural candidate for the feed. It also has the advantage of a relatively broad input impedance bandwidth that can include the entire international unlicensed spectrum from 57 GHz to 66 GHz. Alternative printed feed solutions could also be used: either a passive array of patches or a broadband printed antenna [16] integrated at the base of a tiny hiper-hemispheric lens that would replace the horn inside the air cavity.

An appropriate horn was designed using the CST Microwave Studio™ transient solver [19]. The horn was manufactured in aluminum with 7.8 mm inner aperture diameter, 10 mm flared length and 3.9 mm diameter circular waveguide port (Fig. 3). The horn's aperture dimension was chosen to achieve the desired gain; the flare was adjusted to ensure less than 0.5 mm phase center shift in relation to the horn aperture plane, within the whole band. This shift has negligible effect on the antenna performance.

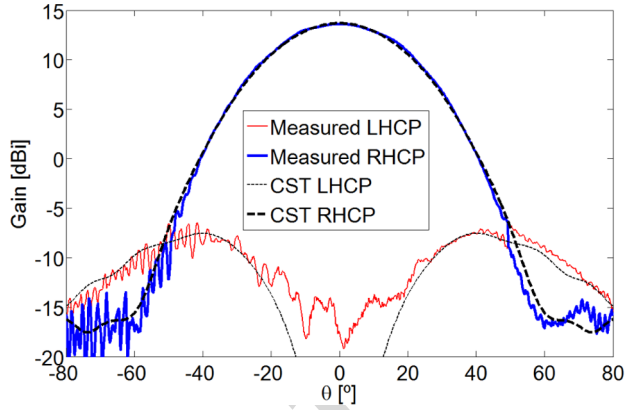

Fig. 4. Measured and simulated co- and cross-polar radiation pattern of the standalone conical horn at 62.5 GHz.

Punctuation mark is missing. Should be "... (RHCP). Fig.4 shows..."

The measured radiation pattern of the standalone horn at 62.5 GHz is represented in Fig. 4. The horn is fed in the TE_{11} mode with right-hand circular polarization (RHCP). Fig. 4 shows a general good agreement between measurements and CST simulation results, both for co- and cross-polarization. The measured gain is 13.6 dBi, which compares very well with the 13.7 dBi CST prediction. For 57 GHz and 66 GHz, CST predicts 13.3 dBi and 14.4 dBi gain, respectively. Also according to the simulation, the radiation efficiency of the horn is above 98% over the entire bandwidth and the $|s_{11}|$ value is always below -20 dB. This is confirmed by measurements.

Pls delete "open"

C. Lens Design and Analysis

The selected material for lens fabrications was polyethylene. Corresponding permittivity and loss tangent values were measured in-house at 62.5 GHz using the well-known open Fabry–Perot open resonator method [20]: $\varepsilon_r = 2.35$ and $\tan(\delta) = 0.0004$. The quite low loss tangent value of polyethylene is favorable for high radiation efficiency of the lens.

The first design step for the extended elliptical lens is to determine the overall lens dimensions required to obtain 20 dBi gain when fed by the manufactured horn. A very fast and relatively accurate design can be achieved using the hybrid Geometric Optics + Physical Optics (GO + PO) lens analysis method [5], [15]. Using the in-house developed software tool (ILASH) [21], it was found that the main axis of the lens generating ellipse should be 13.18 mm and 10 mm, which corresponds to a base radius of 10 mm and a height of 21.8 mm. An 8 mm radius spherical air cavity was then added to the lens. The lens wall was extended 5 mm below the horn aperture to provide fixing points for tilting. With this arrangement the lens can tilt up to $\alpha = 40°$ without hitting the horn. The obtained lens profile is shown in Fig. 2. This lens is onwards referenced as the L1 lens.

Although the GO+PO method is adequate for a first step design and performance evaluation, only a full wave analysis can provide accurate results for this configuration where the lens is small and the feed is so close to the lens. It is important to anticipate namely if the reflected wave at the spherical inner cavity can somehow alter the radiation pattern or the input reflection coefficient of the horn and if reflections at the elliptical interface for the tilted cases do not cause excessive gain scan loss.

Fig. 5. Manufactured L1 lens and feeding horn, assembled in a lab test setup.

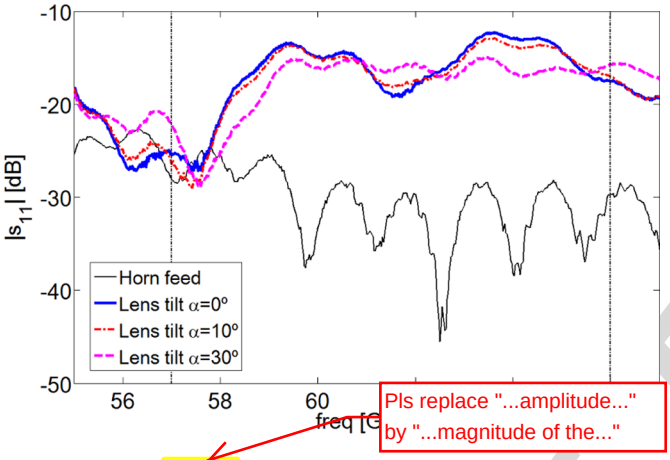

Fig. 6. Measured amplitude input reflection coefficient of the horn when placed in the centre of the spherical air cavity of the L1 lens.

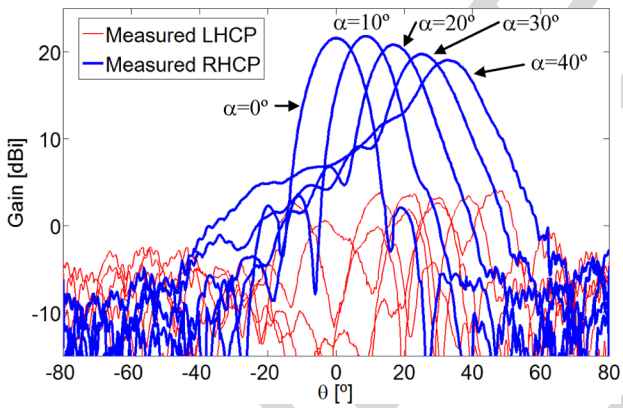

Fig. 7. Measured radiation patterns of the L1 lens antenna for several lens tilt angles α.

Pls replace "...weigh..." by "...weight..."

D. Lens Experimental Results

The CST full-wave simulation results predicted acceptable performance for the designed lens, so it was manufactured. A photograph of the prototype is presented in Fig. 5. Lens weigh is 5 g. A compass was added to the lab setup for easy reading of the manually adjusted lens tilt angles. The rotation of the whole lens assembly about the horn axis for azimuth scan was also done manually. In a final configuration the lens would be tilted by a digitally controlled miniature stepper motor and a second stepper motor would be used for the azimuth scan. The details of the miniaturized automated assembly are out of the scope of the paper.

Measured reflection loss at the horn input port is shown in Fig. 6 versus frequency, for different lens tilt angles. The lens spherical cavity reflects back some radiation into the horn; $|s_{11}|$ clearly increases with the inclusion of the lens. However it stays below -12 dB for all tilt angles, throughout the WirelessHD band. Simulations have shown that a quarter wavelength matching layer at the inner wall of the lens lowers this reflection by about 5 dB. H ion complexity does not justify inal improvement over the already acceptable -12 dB level.

Punctuation mark is missing.
Should be: "...Fig 7. Gain is..."

The lens radiation patterns were measured at 62.5 GHz for different tilt angles in the $\alpha = 0$ to 40° range. Co- and cross-polarization results are presented in Fig. 7 Gain is 21.6 dBi for zero-tilt position and gradually decreases while the beam deforms for increasing lens tilt. It can be noticed though, that the lens preserves the circular polarization of the horn. The cross polarization level in the main beam direction is well below -15 dB for all lens tilts. This is an indication that the reflected wave at the inner spherical cavity does not deteriorate much the horn's radiation pattern and polarization.

Fig. 8 picks two of the previous curves and superimposes the corresponding CST simulated results. The remarkable agreement that can be seen both for the co- and cross-polarization curves was also obtained for every tilt angle, thus entitling to rely on CST simulation results for drawing conclusions ahead for other frequencies in the WirelessHD band.

Lens performance indicators computed from measured results are summarized in Table I versus tilt angle. Gain is above 20 dB for almost all tilt angles, with excellent radiation efficiency values above 96%. Considering 2 dB scan loss as the limit, this lens can reach a beam tilt of 25°, corresponding to 30° lens tilt. Note that contrary to GO prediction, there is an increasing difference between t α_{beam} and the lens tilt angle α happens, in order to set the st a wider scan angle. As lens tilts, the feed illumination gradually exceeds the previously defined $\theta < \theta_{\max}$ region of the lens. According to expression, we obtain $\theta_{\max} = 49°$ for a polyethylene lens. On the other hand, the -10 dB half-beamwidth of the horn radiation (Fig. 4) is $\theta_{-10\text{dB}} = 35°$. Therefore, according to GO, the lens shall be tilted only up to

missing eq. reference number.
Should be
"...to expression (1), we..."

$$\alpha = \theta_{\max} - \theta_{-10\text{dB}} = 14° \tag{2}$$

before part of the feed radiation starts to build side lobes and launches a surface wave along the lens outer interface [22]. Increasing the material permittivity would increase $\theta_{\max}$, but this would also increase the adverse effects of reflected waves over the lenses interfaces. The solution is to use a second refraction surface to try to increase $\theta_{\max}$, an approach that is explored in Section IV.

IV. Solution With Two Refraction Surfaces

A. Design and Analysis

The objective is to design a two refraction surface lens that maximizes the portion of the output lens surface that is able to

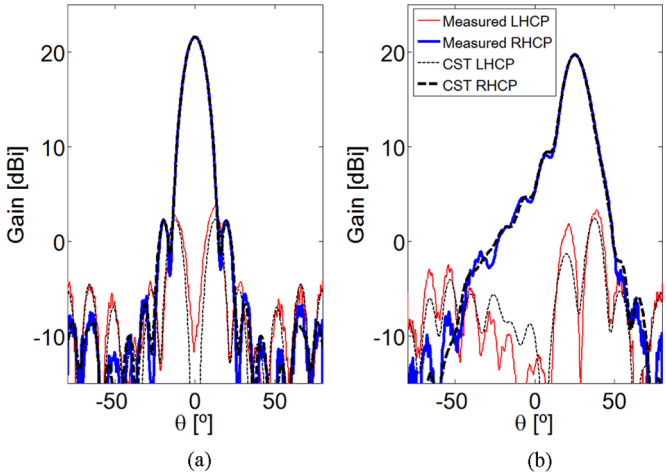

Fig. 8. Measured and simulated radiation pattern of the L1 lens antenna at 62.5 GHz. (a) Lens tilt angle $\alpha = 0°$. (b) Lens tilt angle $\alpha = 30°$.

Pls replace "HIGHER" by "HIGHEST"

TABLE I
MEASURED PERFORMANCE OF THE L1 LENS AT 62.5 GHZ VERSUS LENS TILT α. α_{beam} INDICATES THE MAIN BEAM DIRECTION, ΔG IS THE GAIN SCAN LOSS, XPOL IS THE HIGHER CROSS POLARIZATION LEVEL IN THE MAIN BEAM FULL WIDTH AT -10 dB AND η IS THE CST SIMULATED RADIATION EFFICIENCY

L1 Lens					
α	α_{beam}	G (dBi)	ΔG (dB)	XPol (dB)	η (%)
0º	0.0º	21.6	0.2	-18.5	96.1
10º	8.9º	21.8	0.0	-18.5	96.6
20º	17.3º	20.9	0.9	-17.6	96.7
30º	25.6º	19.7	2.1	-16.4	97.0
40º	32.5º	19.1	2.7	-14.9	97.5

collimate the horn's radiation. This is equivalent to increasing the lens $\theta_{\max}$ value. The two lens interfaces play a role to broaden this maximum angle.

Consider the geometry of Fig. 9. Using Snell refraction law at the bottom lens interface leads to

$$\frac{\partial r(\theta)}{\partial \theta} = \frac{\sqrt{\varepsilon_r}\sin[\theta - \gamma(\theta)]}{\sqrt{\varepsilon_r}\cos[\theta - \gamma(\theta)] - 1} r(\theta) \tag{3}$$

where θ is the independent variable. On the other hand, by imposing an electrical path length condition, we get

$$F + \sqrt{\varepsilon_r}\, T = r(\theta) + \sqrt{\varepsilon_r}\, l(\theta) + s(\theta) \tag{4}$$

where

$$s(\theta) = F + T - r(\theta)\cos(\theta) - l(\theta)\cos[\gamma(\theta)]. \tag{5}$$

F and T are input constants, whereas $r(\theta)$, $l(\theta)$ and $\gamma(\theta)$ are unknown functions. A third design condition is required to define a unique solution. For that we write $r(\theta)$ analytically as a Taylor series expansion in θ

$$r(\theta) = \sum_{n=0}^{8} C_n \theta^n. \tag{6}$$

Missing $\partial r/\partial\theta = 0$

So the left-hand side of (3) can also be written analytically. We set $C_0 = F$ and $C_1 = 0$ in order to impose at $\theta = 0°$; this ensures null refraction for the central ray. Coefficients C_2 to C_8 are generated by using the genetic algorithm (GA) optimization method as detailed next. Setting the C_n coefficients defines the $r(\theta)$ function in (6) so $\gamma(\theta)$ can be calculated from (3) and then $l(\theta)$ can be calculated from (4) and (5). The latter functions define the lens upper surface.

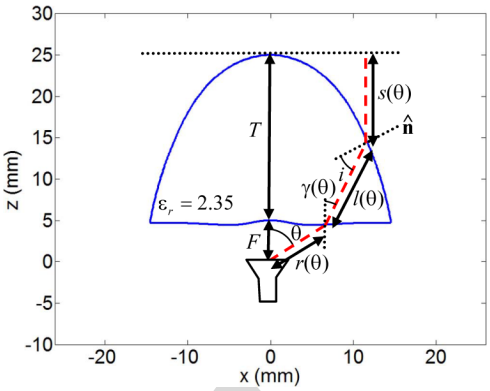

Fig. 9. Geometry for the design of two-refraction surface collimated beam lens.

As mentioned, the above formulation is integrated with a GA loop to test different shapes of the bottom lens surface $r(\theta)$, with the goal to maximize the $\theta_{\max}$ angle of the lens, subject to the following constraints:

a) $r(\theta) > 4.5$ mm, to ensure that the edges of the horn never touch the bottom lens surface when the lens is tilted.
b) The bottom lens surface cannot cross the upper surface except at the edge of the lens.
c) Ray incidence angle at the upper lens interface must be below 95% of the critical angle i_c.

This latter constrain minimizes the excitation of a lateral wave [22] along the lens upper surface. This can happen when ray's incidence angle i, measured with respect to lens local normal $\hat{\mathbf{n}}$, approaches the total reflection condition

$$i \geq i_c = a\sin\left(\frac{1}{\sqrt{\varepsilon_r}}\right) = 40.7°. \tag{7}$$

As previously referred, the surface wave tends to deflect part of the lens radiation away from the main beam direction reducing the directivity.

The above process was run considering $F = 5$ mm and $T = 20$ mm to obtain a lens with similar size as the elliptical one. The lens material is polyethylene. The best lens solution was found for

$$r(\theta) = 0.0274\theta^8 + 0.7683\theta^7 + 0.4522\theta^6 + 0.2553\theta^5 + 0.3774\theta^4 + 0.7369\theta^3 + 0.7353\theta^2 + 5$$

resulting in the lens profile presented in Fig. 9. This lens presents a $\theta_{\max}$ value of 72°, much wider than the 49° of the elliptical lens. The bottom lens surface no longer surrounds the feed and therefore it is mechanically possible to tilt the lens for much wider angles then in the previous case. The base radius of this lens is 29.4 mm. After GO design, the actual lens performance was evaluated using CST. The obtained performance, in accordance with specifications, is presented in the next section. This solution is onward referenced as the L2 lens.

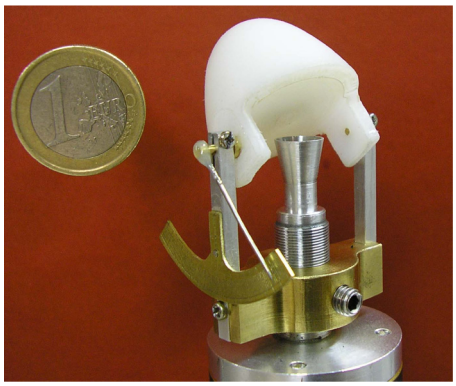

Fig. 10. Photograph of the manufactured L2 lens plus horn feed.

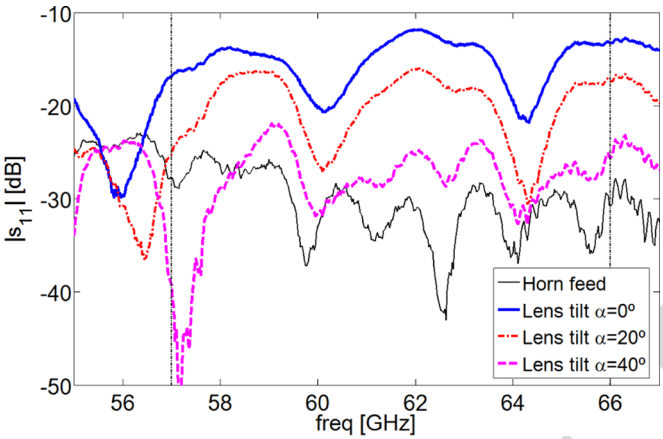

Fig. 11. Measured amplitude input reflection coefficient of the horn when placed in the phase centre of the L2 lens.

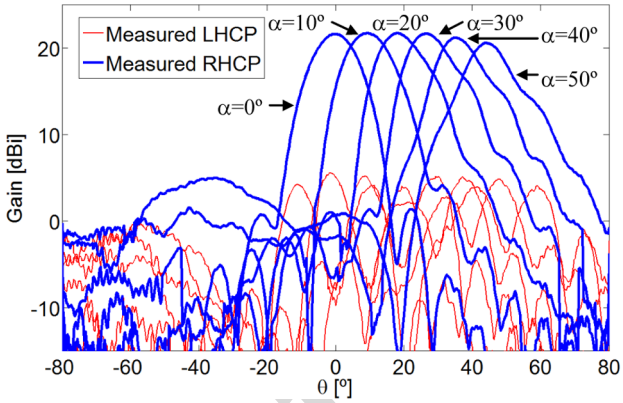

Fig. 12. Measured radiation patterns of the L2 lens antenna for several lens tilt angles α.

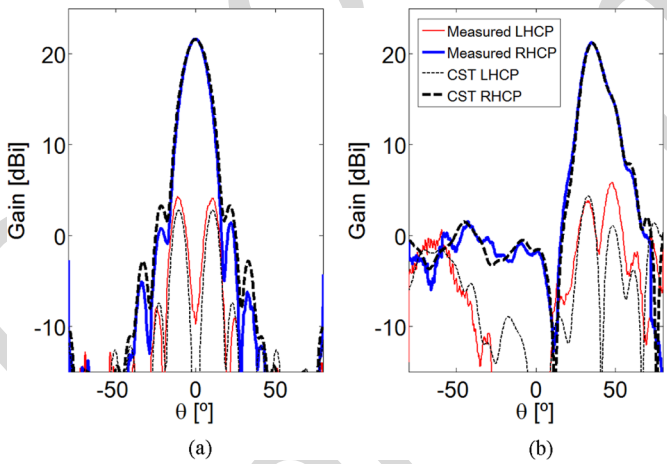

Fig. 13. Measured and simulated radiation pattern of the L2 lens antenna at 62.5 GHz. (a) Lens tilt angle $\alpha = 0°$. (b) Lens tilt angle $\alpha = 40°$.

B. Measurements

The L2 lens has been fabricated and a photograph is shown in Fig. 10; its weight is 8 g. In this case the lens tilting axis lies outside the lens volume, so two lateral extensions of the same lens material (polyethylene) were added to provide fixing points for lens tilting. These extensions are not illuminated by the horn main lobe, so they do not affect the lens radiation pattern.

The measured return loss at the horn input port is presented in Fig. 11. Now $|s_{11}|$ decreases with lens tilt since the slight reflected wave at the bottom of the lens is deflected way from the horn aperture, unlike the previous lens with spherical inner cavity.

The measured co-polarization radiation patterns of the L2 lens are presented in Fig. 12 for 62.5 GHz. The presented curves correspond to 10° steps of the lens tilt angle in the $\alpha = 0$ to 50° range. L2 presents considerable lower scanning loss than the L1 lens and also presents a much better defined main beam up to a maximum scan angle of 45°. The observed beam deformation with tilt angle is not critical for the WirelessHD application since the gain scan loss is negligible.

Like what was done for the elliptical lens, in Fig. 13 two of the previous curves are superimposed on the CST prediction to show the excellent agreement. Similar agreement was obtained for the other tilt angles, which once again validates the simulation model and enables its use ahead for the analysis of other frequencies in the WirelessHD band.

The L2 performance indicator values are summarized in Table II. The measured gain, in the order of 21.7 dB, is remarkably stable with lens tilt and this behavior is extended up to 50° tilt; corresponding beam direction is near 45°, almost doubling the maximum scan angle of the L1 lens, considering the same 2 dB scan loss criteria. Furthermore, the lens ensures considerable low cross polarization level for all tilt angles and the radiation efficiency is above 95%.

CST simulations have shown that the L2 lens performance is also very stable across the entire WirelessHD frequency band, with only ± 1 dB gain variation (Fig. 14).

Additional simulations were performed to determine the possible improvement of adding a quarter wavelength matching layer at the bottom lens surface [23]. The resulting reduction of $|s_{11}|$ at the horn input port is noticeable only for near-zero lens tilts; $|s_{11}|$ lowers by 5 dB and gain improves by $+0.6$ dB. However, for increasing tilt angles, this minor improvement decreases and even reaches -0.4 dB gain reduction for 50° lens tilt. This effect is observed since the matching layer depth is constant, equal to $\lambda_d/4 = 0.969$ mm, and therefore it performs better for near to normal incidence, which is not the case for large lens tilts.

Simulations were performed also for the case where the matching layer was extended to the upper surface, completely

Pls replace by "HIGHEST"

TABLE II
MEASURED PERFORMANCE INDICATOR VALUES OF THE L2 LENS AT 62.5 GHZ VERSUS LENS TILT α. α_{beam} INDICATES THE MAIN BEAM DIRECTION, ΔG IS THE SCAN LOSS VALUE, XPOL IS THE HIGHER CROSS POLARIZATION LEVEL IN THE MAIN BEAM FULL WIDTH AT -10 dB AND η IS THE CST SIMULATED RADIATION EFFICIENCY

L2 Lens					
α	α_{beam}	G (dBi)	ΔG (dB)	XPol (dB)	η (%)
0º	0.0º	21.7	0.0	-17.3	95.3
10º	9.7º	21.7	0.0	-16.2	95.5
20º	19.5º	21.7	0.0	-16.5	95.4
30º	27.9º	21.7	0.0	-16.5	95.8
40º	36.4º	21.2	0.5	-16.4	96.0
50º	44.8º	20.6	1.1	-16.5	97.0

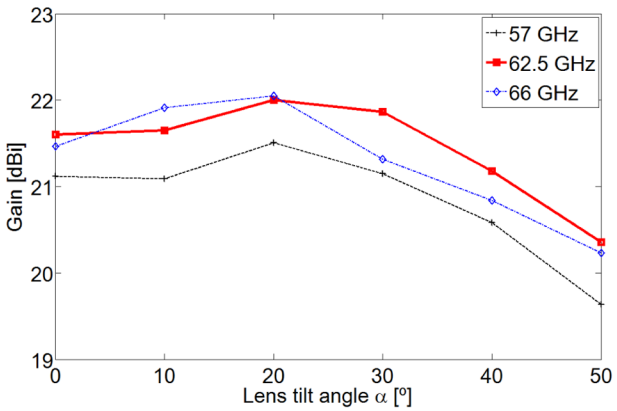

Fig. 14. Gain variation of the L2 lens versus tilt angle computed for three frequencies within the WirelessHD band.

surrounding the lens. In this case the improvement in gain is $+1.3$ dB for the non-tilted case, however it decreases with lens tilt down to -0.3 dB for 50° lens tilt.

In summary, although the matching layer improves the lens gain by more than 1 dB, the gain scan loss characteristic slightly degrades. But, above all, the additional manufacturing complexity of including a matching layer is not worth given the already excellent performance of the L2 lens without matching layer.

V. CONCLUSION

This paper introduced a simple, compact and low-cost antenna solution to perform total mechanical beam steering in the 60-GHz WirelessHD band, intended preferably for a fixed terminal like the flat TV screen. The beam steering is obtained by pivoting an appropriately shaped dielectric lens in front of a single fixed feed. The fabricated lens assembly demonstrated $-45°$ to $+45°$ elevation scan capability over full azimuth, with better than -1.1 dB gain scan loss and radiation efficiency always above 95%. Circular polarization is used to minimize polarization mismatch that can occur in line-of-sight links with linear polarization portable equipment, but the same concept was also tested with similar performance using linear polarization.

The polyethylene lens weights only 8 g; this is a favorable attribute for mechanical steering. The lens can be produced with insignificant cost using molding technique.

Pls add here the following: "These characteristics and the good results led us to patent the antenna [24]".

Pls replace by "deteriorate"

Pls replace by "careful"

Higher beam tilt angles can be obtained by using higher permittivity materials. However, a carefully study is required to evaluate how the more intense reflections at the lens interfaces will deteriorated the overall lens performance and how the inclusion of matching layers can help in this case.

The presented antenna solution can be readily adjusted for other candidate application: the High Altitude Platform System (HAPS) application. In fact, changing the operating frequency is straight forward, involving almost only scaling of the complete solution. A different desired gain can be achieved just by changing the lens overall size.

ACKNOWLEDGMENT

The authors acknowledge the collaboration from V. Fred for prototype construction, and A. Almeida for prototype measurements.

REFERENCES

[1] R. Daniels and R. Heath, Jr, "60 GHz wireless communications: Emerging requirements and design recommendations," *IEEE Veh. Technol. Mag.*, vol. 2, no. 3, pp. 41–50, Sep. 2007.
[2] WirelessHD Specification Version 1.0 Overview, 2007 [Online]. Available: http://www.wirelesshd.org/
[3] C. Fernandes, "Shaped dielectric lenses for wireless millimeter-wave communications," *IEEE Antennas Propagat. Mag.*, vol. 41, no. 5, pp. 141–150, Oct. 1999.
[4] C. Fernandes and J. Fernandes, "Performance of lens antennas in wireless indoor millimeter-wave applications," *IEEE Trans. Microw. Theory Tech.*, vol. 47, no. 6, pt. 1, pp. 732–737, Jun. 1999.
[5] C. Fernandes, "Shaped-Beam Antennas," in *Handbook of Antennas in Wireless Communications*, L. Godara, Ed. New York: CRC Press, 2001, ch. 15.
[6] W. Menzel, D. Pilz, and M. A. Tikrit, "Millimeter- wave folded reflector antennas with high gain, low loss, and low profile," *IEEE Antennas Propagat. Mag.*, vol. 44, no. 3, pp. 24–29, Jun. 2002.
[7] V. Fusco, "Mechanical beam scanning reflect array," *IEEE Trans. Antennas Propagat.*, vol. 53, no. 11, pp. 3842–3844, Nov. 2005.
[8] K. Chang and M. L. T. Y. Rodenbeck, "Novel low-cost beam-steering techniques," *IEEE Trans. Antennas Propagat.*, vol. 50, no. 5, pp. 618–627, May 2002.
[9] K. V. Caekenberghe, T. Vaha-Heikkila, G. Rebeiz, and K. Sarabandi, "Ka-band MEMS TTD passive electronically scanned array (ESA)," in *Proc. IEEE APS/URSI Symp.*, Albuquerque, NM, Jul. 2006, pp. 513–516.
[10] A. Tombak and A. Mortazawi, "A novel low-cost beam-steering technique based on the extended-resonance power-dividing method," *IEEE Trans. Microw. Theory Tech.*, vol. 52, no. 2, pp. 664–669, Feb. 2004.
[11] B. Schoenlinner, X. Wu, J. Ebling, G. Eleftheriades, and G. Rebeiz, "Wide-scan spherical-lens antennas for automotive radars," *IEEE Trans. Microw. Theory Tech.*, vol. 50, no. 9, pp. 2166–2175, Sep. 2002.
[12] H. Kawahara, H. Deguchi, M. Tsuji, and H. Shigesawa, "Design of rotational dielectric dome with linear array feed for wide-angle multibeam antenna applications," *Electronics and Communications in Japan, Part 2*, vol. 90, no. 5, pp. 49–57, 2007.
[13] V. Manasson, L. Sadovnik, and R. Mino, "MMW scanning antenna," *IEEE Aerospace Electronic Syst. Mag.*, vol. 11, no. 10, pp. 29–33, Oct. 1996.
[14] A. Peebles, "A dielectric bifocal lens for multibeam antenna applications," *IEEE Trans. Antennas Propagat.*, vol. 36, no. 5, pp. 599–606, May 1988.
[15] D. Filipovic, S. Gearhart, and G. Rebeiz, "Double-slot antennas on extended hemispherical and elliptical silicon dielectric lenses," *IEEE Trans. Microw. Theory Tech.*, vol. 41, no. 10, pp. 1738–1749, Oct. 1993.
[16] J. Costa and C. Fernandes, "Broadband slot feed for integrated lens antennas," *IEEE Antennas Wireless Propagat. Lett.*, vol. 6, pp. 396–400, Sep. 2007.
[17] G. Godi, R. Sauleau, and D. Thouroude, "Performance of reduced size substrate lens antennas for millimetre-wave communications," *IEEE Trans. Antennas Propagat.*, vol. 53, no. 4, pp. 1278–1286, Apr. 2005.

[18] J. Costa, C. Fernandes, G. Godi, R. Sauleau, L. L. Coq, and H. Legay, "Compact Ka-band lens antennas for LEO satellites," *IEEE Trans. Antennas Propagat.*, vol. 56, no. 6, pp. 1251–1268, May 2008.
[19] Computer Simulation Technology, CST, 2008 [Online]. Available: http://www.cst.com/
[20] L. Chen, C. Ong, C. Neo, V. Varadan, and V. Varadan, *Microwave Electronics: Measurement and Materials Characterization*. London, U.K.: Wiley, 2004.
[21] E. Lima, J. Costa, M. Silveirinha, and C. Fernandes, "ILASH—Software tool for the design of integrated lens antennas," in *Proc. IEEE APS/URSI Symp.*, San Diego, CA, Jul. 2008.
[22] D. Pasqualini and S. Maci, "High-frequency analysis of integrated dielectric lens antennas," *IEEE Trans. Antennas Propagat.*, vol. 52, no. 3, pp. 840–847, Mar. 2004.
[23] M. van der Vorst, P. de Maagt, and M. Herben, "Effect of internal reflections on the radiation properties and input admittance of integrated lens antennas," *IEEE Trans. Microw. Theory Tech.*, vol. 47, no. 9, pp. 1696–1704, Sep. 1999.

Pls add here:
"[24] J. Costa, C. Fernandes and E. Lima, "Compact antenna with mechanical beam steering for tracking wireless mobile communications terminals" (in Portuguese), Patent # PT 104108, June 2008."

Ph.D. degrees in electrical engineering from the Instituto Superior Técnico, Lisbon, Portugal, in 1997 and 2002, respectively.

He is currently a Researcher at the Instituto de Telecomunicações, Lisbon, Portugal. He is also an Assistant Professor at the Departamento de Ciências e Tecnologias da Informação, Instituto Superior de Ciências do Trabalho e da Empresa. His present research interests include lenses, reconfigurable antennas, MEMS switches, UWB and RFID antennas.

Eduardo B. Lima was born in Viseu, Portugal, in 1978. He received the Licenciado degree in electrical engineering from the Instituto Superior Técnico, Lisbon, Portugal, in 2003. He is a Researcher at the Instituto de Telecomunicações, Lisbon, Portugal, and he is currently working toward the M.Sc. degree in electrical engineering at the Instituto Superior Técnico.

From 2004 to 2007, he was involved on the ESA/ESTEC project ILASH (Integrated Lens Antenna Shaping). His present research interests include lenses and reflectors for focused systems.

Carlos A. Fernandes (S'86–M'89–SM'08) received the Licenciado, M.Sc., and Ph.D. degrees in electrical and computer engineering from Instituto Superior Técnico (IST), Technical University of Lisbon, Lisbon, Portugal, in 1980, 1985, and 1990, respectively.

He joined the IST in 1980, where he is presently a Full Professor in the Department of Electrical and Computer Engineering in the areas of microwaves, radio wave propagation and antennas. He is a Senior Researcher at the Instituto de Telecomunicações and coordinator of its Wireless Communications scientific area. He has been the leader of antenna activities in National and European Projects as RACE 2067—MBS (Mobile Broadband System), ACTS AC230—SAMBA (System for Advanced Mobile Broadband Applications) and ESA/ESTEC—ILASH (Integrated Lens Antenna Shaping). He has co-authored a book, a book chapter, and more than 100 technical papers in international journals and conference proceedings, in the areas of antennas and radiowave propagation modeling. His current research interests include dielectric antennas for millimeter wave applications, antennas and propagation modeling for personal communication systems, artificial dielectrics and metamaterials.

Compact Beam-Steerable Lens Antenna for 60-GHz Wireless Communications

Jorge R. Costa, *Member, IEEE*, Eduardo B. Lima, and Carlos A. Fernandes, *Senior Member, IEEE*

***Abstract*—This paper presents a new concept of steerable beam antenna composed by a dielectric lens which pivots in front of a single stationary moderate gain feed. The lens not only allows steering mechanically the beam in elevation and full azimuth, but further increases the gain up to 21 dBi. The solution is broadband, including the entire international unlicensed spectrum from 57 GHz to 66 GHz. A fabricated prototype shows the possibility of tilting the beam from -45° to $+45^\circ$ for all azimuths with gain scan loss below 1.1 dB and radiation efficiency above 95%. The arrangement is very simple, it does not require rotary joints, it is low cost and compact, lens plus feed volume being of the order of $3 \times 3 \times 3$ cm^3 with lens weight less than 10 g.**

***Index Terms*—Compact lens antennas, 60-GHz wireless communication, low-cost, mechanical beam-steering.**

I. Introduction

RECENTLY a new emerging wireless communication standard is being developed to use the world unlicensed spectrum from 57 GHz to 66 GHz [1], [2]. Those frequencies can support very high bit-rate transmission; however, atmospheric impairments limit radio link range to a few hundred meters. Therefore, a new wireless high definition entertaining network (WirelessHD) is being developed for this band to provide indoor communication between terminals requiring high bit-rates, like connecting the Blue Ray recorder, a portable high-definition (HD) game console or a camcorder to a full HD flat screen. To improve the link budget and ensure acceptable system performance and range, antennas with gains greater than 14 dBi or even 20 dBi are required. As a result of the inherent narrow beam, steerable beam capability is envisaged to automatically point the main beam to the direction of a transmitting device or even to follow a moving portable device. Other strategies were explored in the past for similar requirements resorting to constant flux shaped beams without restricting the mobility [3]–[5], but the new emerging standard is pointing in the direction of beam-steered antenna solutions. Antenna compactness and low-cost are of course desirable features for WirelessHD applications.

Manuscript received June 25, 2008; revised September 27, 2008. First published August 04, 2009; current version published October 07, 2009.

J. R. Costa is with the Instituto de Telecomunicações, IST, 1049-001 Lisboa, Portugal, and also with the Instituto Superior de Ciências do Trabalho e da Empresa, Departamento de Ciências e Tecnologias da Informação, 1649-026 Lisboa, Portugal (e-mail: Jorge.Costa@lx.it.pt).

E. B. Lima and C. A. Fernandes are with the Instituto de Telecomunicações, IST, 1049-001 Lisboa, Portugal.

Color versions of one or more of the figures in this paper are available online at http://ieeexplore.ieee.org.

Digital Object Identifier 10.1109/TAP.2009.2029288

Beam-steering can be performed mechanically by moving all or some part of the antenna [6]–[8], electrically by using phased array antennas or switched multiple feed antennas [9]–[11], or by combining the two techniques. Electrical steering has the advantage of being faster than mechanical solutions however, at millimeter waves, efficiency, phase stability and cost are quite critical issues for phased arrays, especially when using MMIC technology to reach mass applications. These issues are being tackled, but as an example, the Ka band antenna implementation reported in [9], using RF MEMS as time delay units for the phasing circuit of a 1×8 element array, presents efficiency of the order of 25% yielding 10 dBi gain. Scanning is in one plane only. Other approach combining a constrained lens with a dome lens is reported in [12], but again the obtained gain is of the order of 10 dBi for a 10λ diameter radome.

Imaginative solutions are reported for mechanical steering that could be appropriate for low-cost implementation at millimeter waves. In [7] a reflectarray is presented that is formed by $1 \times$ N array of rotating circular disks shorted at the periphery. For circular polarized wave incidence, the direction of the reflected beam is controlled by the difference of rotating speeds of the disks. In [13], a solution is presented, based on cylinder metal grating that spins close to two dielectric waveguides perturbing the propagation of the evanescent wave along the waveguide thus controlling its diffraction. The scanning angle is however dependent on frequency and scanning is in one plane. In [8] a similar concept is presented using a different geometry, but with the same inconvenient.

This paper adopts a mechanical steering approach that does not suffer from previous limitations, intended for the antenna that is mounted for instance in the HD screen, as a low-cost and efficient compromise solution for slower racking situations that are most common when pointing in the direction of a HD equipment in the room that is still or is held by a person. Indicative specifications taken here for proof of concept are: > 20 dBi gain steerable-beam, $> 40^\circ$ elevation beam tilt with gain scan loss < 2 dB, full azimuth scan, and radiation efficiency $> 95\%$; furthermore, the antenna is required to be compact, simple and adequate for low-cost mass production.

The proposed antenna solution consists of an axial symmetric dielectric lens that pivots with a simple two axis movement in front of a moderate directivity stationary feed. The lens main function is to tilt the beam with respect to the fixed feed axis, within a wide conic angular sector. The lens is used also to collimate the beam in order to push the gain up to more than 20 dBi. These two functions require appropriate shaping of the top and bottom lens surfaces, which is the key factor for the usefulness of the proposed solution. The resulting antenna assembly is simple, it is reasonably small with wide-angle scanning; the lens

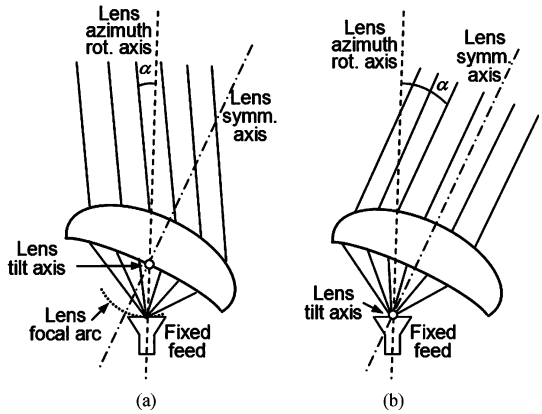

Fig. 1. Two axis pivoting lens placed in front of a fixed feed for beam-steering. (a) Lens tilt axis centered with respect to its focal arc. (b) Tilt axis passing through lens focal point.

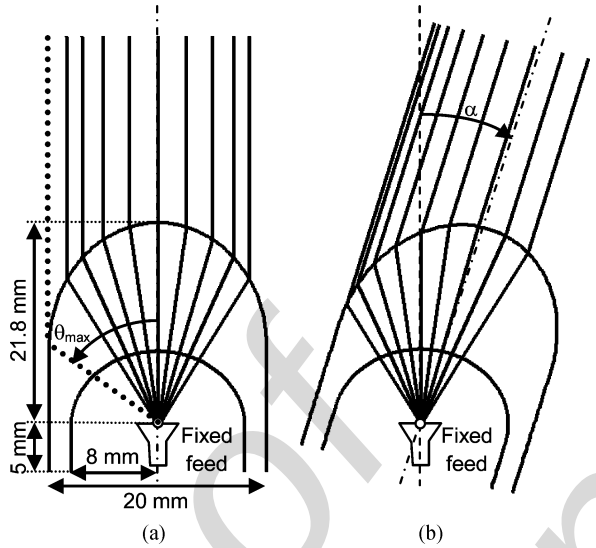

Fig. 2. Ray tracing in polyethylene elliptical lens with spherical air cavity. (a) zero-tilt case. (b) $\alpha = 15^\circ$ lens-tilt.

can be fabricated using a molding process. The feed is intentionally chosen to be stationary, in order to dispense expensive and fault prone millimeter-wave rotary joints. All these characteristics favor the objective of a very low-cost solution.

This is opposed to the classical concept of scanning lenses where the lens is stationary and a cluster of feeds is distributed over the lens focal arc [14]. Any of these or other reported mechanical steering antennas are more complex, larger and more costly at millimeter waves than our proposed solution.

This paper is organized as follows. The antenna concept is presented in Section II. The design and performance of a lens solution with a single refraction surface are presented in Section III. Section IV presents an improved lens solution with two refraction surfaces. In both cases, numerical and experimental results are given and discussed. Conclusions are finally drawn in Section V.

II. Concept Description

The challenge here is to comply with the previously referred specifications using just one pivoting element in front of the fixed feed, to keep with a very simple and reliable structure.

One obvious possibility would be to place a conventional scanning lens in front of the stationary feed and tilt the lens in such a way that its focal arc always contained the feed phase center [Fig. 1(a)]. However, it can be shown that the resulting maximum scanning angle α is very limited in this case.

The approach in this paper is to tilt a collimated beam lens about its central focal point [Fig. 1(b)]; this makes all the difference. In this way the lens does not need to comply with a scanning beam condition, which thus leaves more degrees of freedom for lens profile optimization. Being a collimated beam lens with centered feeding, the output rays always emerge parallel to the lens symmetry axis, making the α beam tilt angle to be the same as the lens tilt angle. The azimuth beam scanning is obtained by simultaneous rotation of the lens about the feed axis.

The issues to consider when designing the collimated beam lens are the maximum achievable beam tilt angle, the maximum gain and the minimum gain scan loss. These characteristics are determined by the lens profile of course, but they are in part limited by reflections at the dielectric interfaces and by feed illumination spillover as lens tilt increases. An appropriate feed must be designed for proper lens illumination.

Two lens geometries are presented: one is based on a single refraction surface configuration that is used for easy explanation of the concept and its limitations; the second lens, based on double-refraction lens, is optimized to tackle those limitations and present improved performance.

III. Solution With Single Refraction Surface

A. Lens Configuration

The elliptical lenses are common solutions to obtain collimated beams [15]–[17]: rays departing from the feed immersed in the dielectric at the ellipse focal point emerge from the lens surface parallel to the lens axis. For low loss dielectric materials, the lens antenna gain is mostly determined by its aperture size.

In order to be able to tilt the lens without tilting the feed, it must be detached from the lens. Using the same approach that the authors adopted for a LEO satellite lens application [18], a spherical air dome can be opened at the base of the lens, centered with the feed phase centre (Fig. 2). The spherical cavity does not introduce major modifications to the feed's illumination of the lens elliptical surface since the lens inner interface does not produce any refraction. In this way the lens can tilt and steer the beam in elevation, while the feed remains stationary at the focal point.

Fig. 2 shows a ray tracing in an extended hemi-elliptical lens with inner air cavity for two lens tilts. It illustrates that the output rays always emerge parallel to the lens axis, and so the beam tilt is the same as the lens tilt. For any lens tilt, the lens can rotate about the feed axis to produce an azimuth beam scan.

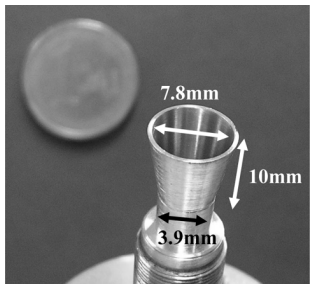

Fig. 3. Photograph of the manufactured circular horn feed.

It is noted that the subtended angle of the feed radiation θ must be restricted in order to avoid that peripheral rays exceed the lens collimating region. Based upon Geometrical Optics (GO), the collimating region corresponds to

$$\theta < \theta_{\max} = \operatorname{acos}\left(\frac{1}{\sqrt{\varepsilon_r}}\right) \tag{1}$$

where ε_r is the lens material permittivity and θ is the angle between a ray path departing from the feed and the lens axis; $\theta_{\max}$ value corresponds to the first ray that hits the external cylinder wall of the lens. For larger angles, rays are refracted away from the main beam direction, contributing to side lobes and to lowering gain. For a given feed, the impact of this effect is higher as the lens tilt increases, originating gain scan loss.

B. Circular Horn Feed

The feed must be designed such that its radiation is negligible at $\theta_{\max}$ for the maximum lens tilt, which points to a moderate directivity feed radiation pattern. A compromise is also needed with the feed aperture size to fit into the spherical air cavity at the focal point and further allow space for lens tilting without being impaired by the feed. Calculations showed that feed directivity in the range 13–14 dBi is adequate for the envisaged lenses.

As for polarization, considering that the equipment at the other end of the link is potentially portable, circular polarization (CP) was preferred here over linear polarization. Anyway, the concept remains valid and feasible for linear polarization.

Given the above, a conical horn antenna is a natural candidate for the feed. It also has the advantage of a relatively broad input impedance bandwidth that can include the entire international unlicensed spectrum from 57 GHz to 66 GHz. Alternative printed feed solutions could also be used: either a passive array of patches or a broadband printed antenna [16] integrated at the base of a tiny hiper-hemispheric lens that would replace the horn inside the air cavity.

An appropriate horn was designed using the CST Microwave Studio™ transient solver [19]. The horn was manufactured in aluminum with 7.8 mm inner aperture diameter, 10 mm flared length and 3.9 mm diameter circular waveguide port (Fig. 3). The horn's aperture dimension was chosen to achieve the desired gain; the flare was adjusted to ensure less than 0.5 mm phase center shift in relation to the horn aperture plane, within the whole band. This shift has negligible effect on the antenna performance.

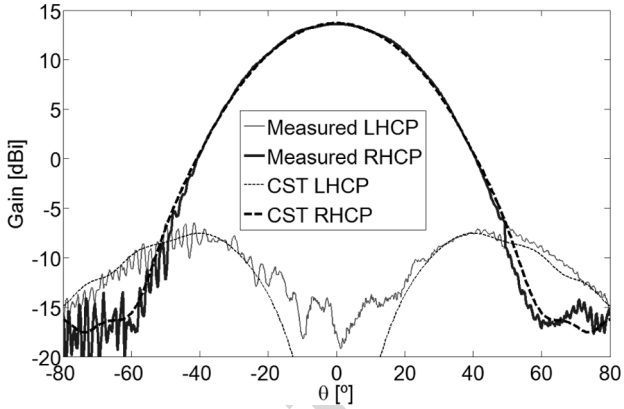

Fig. 4. Measured and simulated co- and cross-polar radiation pattern of the standalone conical horn at 62.5 GHz.

The measured radiation pattern of the standalone horn at 62.5 GHz is represented in Fig. 4. The horn is fed in the TE_{11} mode with right-hand circular polarization (RHCP) Fig. 4 shows a general good agreement between measurements and CST simulation results, both for co- and cross-polarization. The measured gain is 13.6 dBi, which compares very well with the 13.7 dBi CST prediction. For 57 GHz and 66 GHz, CST predicts 13.3 dBi and 14.4 dBi gain, respectively. Also according to the simulation, the radiation efficiency of the horn is above 98% over the entire bandwidth and the $|s_{11}|$ value is always below -20 dB. This is confirmed by measurements.

C. Lens Design and Analysis

The selected material for lens fabrications was polyethylene. Corresponding permittivity and loss tangent values were measured in-house at 62.5 GHz using the well-known open Fabry–Perot open resonator method [20]: $\varepsilon_r = 2.35$ and $\tan(\delta) = 0.0004$. The quite low loss tangent value of polyethylene is favorable for high radiation efficiency of the lens.

The first design step for the extended elliptical lens is to determine the overall lens dimensions required to obtain 20 dBi gain when fed by the manufactured horn. A very fast and relatively accurate design can be achieved using the hybrid Geometric Optics + Physical Optics (GO + PO) lens analysis method [5], [15]. Using the in-house developed software tool (ILASH) [21], it was found that the main axis of the lens generating ellipse should be 13.18 mm and 10 mm, which corresponds to a base radius of 10 mm and a height of 21.8 mm. An 8 mm radius spherical air cavity was then added to the lens. The lens wall was extended 5 mm below the horn aperture to provide fixing points for tilting. With this arrangement the lens can tilt up to $\alpha = 40°$ without hitting the horn. The obtained lens profile is shown in Fig. 2. This lens is onwards referenced as the L1 lens.

Although the GO+PO method is adequate for a first step design and performance evaluation, only a full wave analysis can provide accurate results for this configuration where the lens is small and the feed is so close to the lens. It is important to anticipate namely if the reflected wave at the spherical inner cavity can somehow alter the radiation pattern or the input reflection coefficient of the horn and if reflections at the elliptical interface for the tilted cases do not cause excessive gain scan loss.

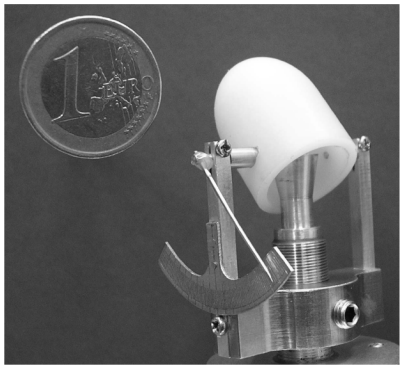

Fig. 5. Manufactured L1 lens and feeding horn, assembled in a lab test setup.

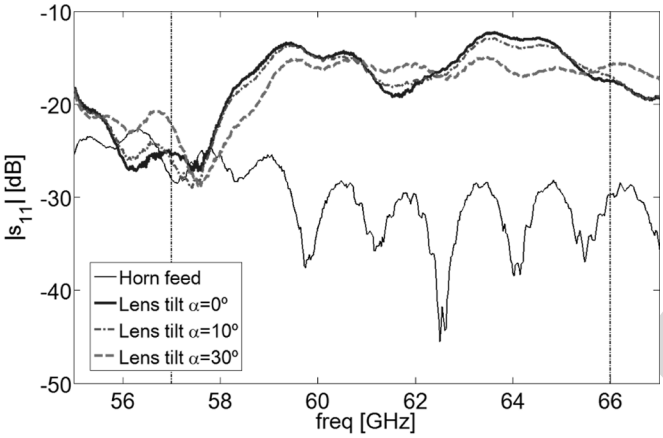

Fig. 6. Measured amplitude input reflection coefficient of the horn when placed in the centre of the spherical air cavity of the L1 lens.

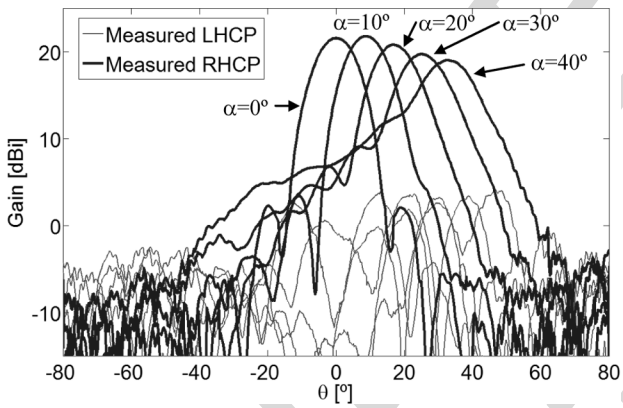

Fig. 7. Measured radiation patterns of the L1 lens antenna for several lens tilt angles α.

D. Lens Experimental Results

The CST full-wave simulation results predicted acceptable performance for the designed lens, so it was manufactured. A photograph of the prototype is presented in Fig. 5. Lens weigh is 5 g. A compass was added to the lab setup for easy reading of the manually adjusted lens tilt angles. The rotation of the whole lens assembly about the horn axis for azimuth scan was also done manually. In a final configuration the lens would be tilted by a digitally controlled miniature stepper motor and a second stepper motor would be used for the azimuth scan. The details of the miniaturized automated assembly are out of the scope of the paper.

Measured reflection loss at the horn input port is shown in Fig. 6 versus frequency, for different lens tilt angles. The lens spherical cavity reflects back some radiation into the horn; $|s_{11}|$ clearly increases with the inclusion of the lens. However it stays below -12 dB for all tilt angles, throughout the WirelessHD band. Simulations have shown that a quarter wavelength matching layer at the inner wall of the lens lowers this reflection by about 5 dB. However the associated fabrication complexity does not justify its use considering the marginal improvement over the already acceptable -12 dB level.

The lens radiation patterns were measured at 62.5 GHz for different tilt angles in the $\alpha = 0$ to 40° range. Co- and cross-polarization results are presented in Fig. 7 Gain is 21.6 dBi for zero-tilt position and gradually decreases while the beam deforms for increasing lens tilt. It can be noticed though, that the lens preserves the circular polarization of the horn. The cross polarization level in the main beam direction is well below -15 dB for all lens tilts. This is an indication that the reflected wave at the inner spherical cavity does not deteriorate much the horn's radiation pattern and polarization.

Fig. 8 picks two of the previous curves and superimposes the corresponding CST simulated results. The remarkable agreement that can be seen both for the co- and cross-polarization curves was also obtained for every tilt angle, thus entitling to rely on CST simulation results for drawing conclusions ahead for other frequencies in the WirelessHD band.

Lens performance indicators computed from measured results are summarized in Table I versus tilt angle. Gain is above 20 dB for almost all tilt angles, with excellent radiation efficiency values above 96%. Considering 2 dB scan loss as the limit, this lens can reach a beam tilt of 25°, corresponding to 30° lens tilt. Note that contrary to GO prediction, there is an increasing difference between the main beam pointing direction α_{beam} and the lens tilt angle α. It is relevant to explain why this happens, in order to set the strategy for lens redesign aiming at a wider scan angle. As lens tilts, the feed illumination gradually exceeds the previously defined $\theta < \theta_{\max}$ region of the lens. According to expression, we obtain $\theta_{\max} = 49°$ for a polyethylene lens. On the other hand, the -10 dB half-beamwidth of the horn radiation (Fig. 4) is $\theta_{-10\text{dB}} = 35°$. Therefore, according to GO, the lens shall be tilted only up to

$$\alpha = \theta_{\max} - \theta_{-10\text{dB}} = 14° \tag{2}$$

before part of the feed radiation starts to build side lobes and launches a surface wave along the lens outer interface [22]. Increasing the material permittivity would increase $\theta_{\max}$, but this would also increase the adverse effects of reflected waves over the lenses interfaces. The solution is to use a second refraction surface to try to increase $\theta_{\max}$, an approach that is explored in Section IV.

IV. Solution With Two Refraction Surfaces

A. Design and Analysis

The objective is to design a two refraction surface lens that maximizes the portion of the output lens surface that is able to

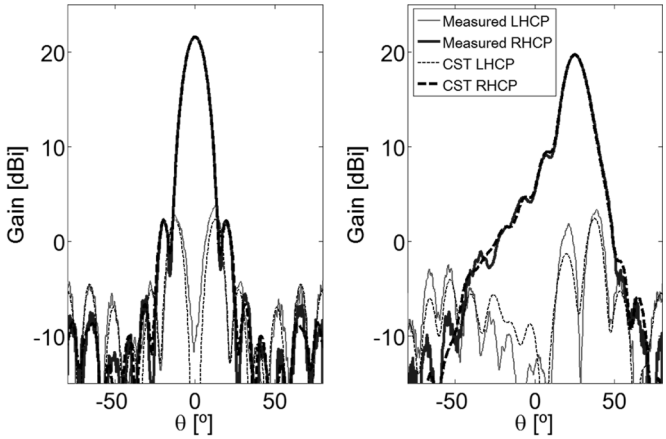

Fig. 8. Measured and simulated radiation pattern of the L1 lens antenna at 62.5 GHz. (a) Lens tilt angle $\alpha = 0°$. (b) Lens tilt angle $\alpha = 30°$.

TABLE I
MEASURED PERFORMANCE OF THE L1 LENS AT 62.5 GHZ VERSUS LENS TILT α. α_{beam} INDICATES THE MAIN BEAM DIRECTION, ΔG IS THE GAIN SCAN LOSS, XPOL IS THE HIGHER CROSS POLARIZATION LEVEL IN THE MAIN BEAM FULL WIDTH AT -10 dB AND η IS THE CST SIMULATED RADIATION EFFICIENCY

L1 Lens					
α	α_{beam}	G (dBi)	ΔG (dB)	XPol (dB)	η (%)
0º	0.0º	21.6	0.2	-18.5	96.1
10º	8.9º	21.8	0.0	-18.5	96.6
20º	17.3º	20.9	0.9	-17.6	96.7
30º	25.6º	19.7	2.1	-16.4	97.0
40º	32.5º	19.1	2.7	-14.9	97.5

collimate the horn's radiation. This is equivalent to increasing the lens $\theta_{\max}$ value. The two lens interfaces play a role to broaden this maximum angle.

Consider the geometry of Fig. 9. Using Snell refraction law at the bottom lens interface leads to

$$\frac{\partial r(\theta)}{\partial \theta} = \frac{\sqrt{\varepsilon_r}\sin[\theta - \gamma(\theta)]}{\sqrt{\varepsilon_r}\cos[\theta - \gamma(\theta)] - 1} r(\theta) \tag{3}$$

where θ is the independent variable. On the other hand, by imposing an electrical path length condition, we get

$$F + \sqrt{\varepsilon_r}\, T = r(\theta) + \sqrt{\varepsilon_r}\, l(\theta) + s(\theta) \tag{4}$$

where

$$s(\theta) = F + T - r(\theta)\cos(\theta) - l(\theta)\cos[\gamma(\theta)]. \tag{5}$$

F and T are input constants, whereas $r(\theta)$, $l(\theta)$ and $\gamma(\theta)$ are unknown functions. A third design condition is required to define a unique solution. For that we write $r(\theta)$ analytically as a Taylor series expansion in θ

$$r(\theta) = \sum_{n=0}^{8} C_n \theta^n. \tag{6}$$

So the left-hand side of (3) can also be written analytically. We set $C_0 = F$ and $C_1 = 0$ in order to impose at $\theta = 0°$; this

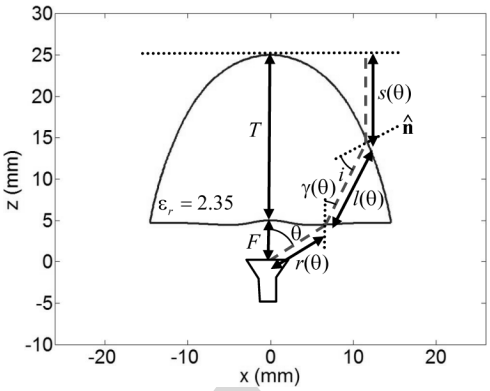

Fig. 9. Geometry for the design of two-refraction surface collimated beam lens.

ensures null refraction for the central ray. Coefficients C_2 to C_8 are generated by using the genetic algorithm (GA) optimization method as detailed next. Setting the C_n coefficients defines the $r(\theta)$ function in (6) so $\gamma(\theta)$ can be calculated from (3) and then $l(\theta)$ can be calculated from (4) and (5). The latter functions define the lens upper surface.

As mentioned, the above formulation is integrated with a GA loop to test different shapes of the bottom lens surface $r(\theta)$, with the goal to maximize the $\theta_{\max}$ angle of the lens, subject to the following constraints:

a) $r(\theta) > 4.5$ mm, to ensure that the edges of the horn never touch the bottom lens surface when the lens is tilted.
b) The bottom lens surface cannot cross the upper surface except at the edge of the lens.
c) Ray incidence angle at the upper lens interface must be below 95% of the critical angle i_c.

This latter constrain minimizes the excitation of a lateral wave [22] along the lens upper surface. This can happen when ray's incidence angle i, measured with respect to lens local normal $\hat{\mathbf{n}}$, approaches the total reflection condition

$$i \geq i_c = a\sin\left(\frac{1}{\sqrt{\varepsilon_r}}\right) = 40.7°. \tag{7}$$

As previously referred, the surface wave tends to deflect part of the lens radiation away from the main beam direction reducing the directivity.

The above process was run considering $F = 5$ mm and $T = 20$ mm to obtain a lens with similar size as the elliptical one. The lens material is polyethylene. The best lens solution was found for

$$r(\theta) = 0.0274\theta^8 + 0.7683\theta^7 + 0.4522\theta^6 + 0.2553\theta^5 + 0.3774\theta^4 + 0.7369\theta^3 + 0.7353\theta^2 + 5$$

resulting in the lens profile presented in Fig. 9. This lens presents a $\theta_{\max}$ value of 72°, much wider than the 49° of the elliptical lens. The bottom lens surface no longer surrounds the feed and therefore it is mechanically possible to tilt the lens for much wider angles then in the previous case. The base radius of this lens is 29.4 mm. After GO design, the actual lens performance was evaluated using CST. The obtained performance, in accordance with specifications, is presented in the next section. This solution is onward referenced as the L2 lens.

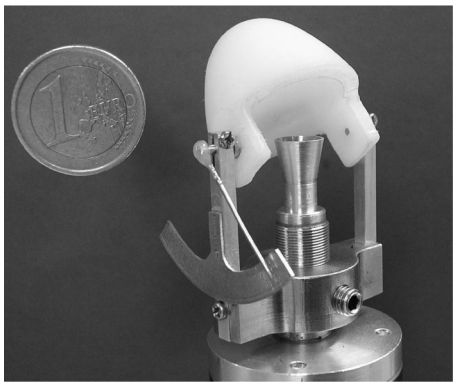

Fig. 10. Photograph of the manufactured L2 lens plus horn feed.

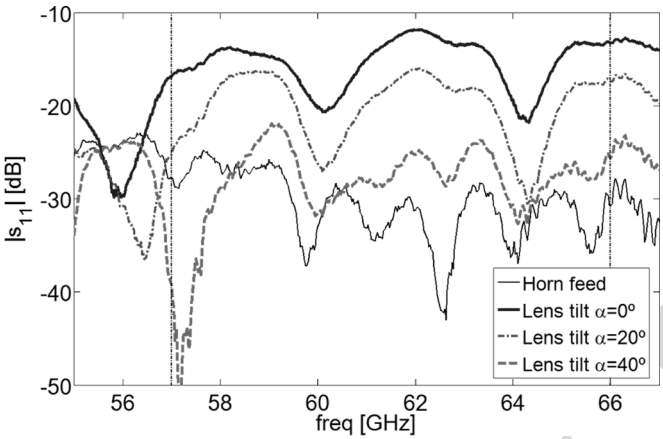

Fig. 11. Measured amplitude input reflection coefficient of the horn when placed in the phase centre of the L2 lens.

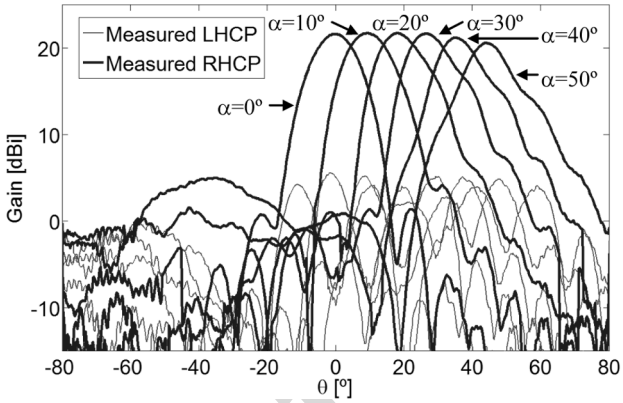

Fig. 12. Measured radiation patterns of the L2 lens antenna for several lens tilt angles α.

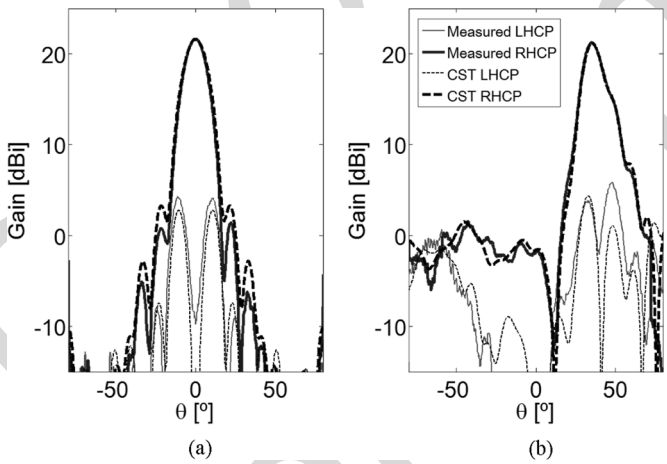

Fig. 13. Measured and simulated radiation pattern of the L2 lens antenna at 62.5 GHz. (a) Lens tilt angle $\alpha = 0°$. (b) Lens tilt angle $\alpha = 40°$.

B. Measurements

The L2 lens has been fabricated and a photograph is shown in Fig. 10; its weight is 8 g. In this case the lens tilting axis lies outside the lens volume, so two lateral extensions of the same lens material (polyethylene) were added to provide fixing points for lens tilting. These extensions are not illuminated by the horn main lobe, so they do not affect the lens radiation pattern.

The measured return loss at the horn input port is presented in Fig. 11. Now $|s_{11}|$ decreases with lens tilt since the slight reflected wave at the bottom of the lens is deflected way from the horn aperture, unlike the previous lens with spherical inner cavity.

The measured co-polarization radiation patterns of the L2 lens are presented in Fig. 12 for 62.5 GHz. The presented curves correspond to 10° steps of the lens tilt angle in the $\alpha = 0$ to 50° range. L2 presents considerable lower scanning loss than the L1 lens and also presents a much better defined main beam up to a maximum scan angle of 45°. The observed beam deformation with tilt angle is not critical for the WirelessHD application since the gain scan loss is negligible.

Like what was done for the elliptical lens, in Fig. 13 two of the previous curves are superimposed on the CST prediction to show the excellent agreement. Similar agreement was obtained for the other tilt angles, which once again validates the simulation model and enables its use ahead for the analysis of other frequencies in the WirelessHD band.

The L2 performance indicator values are summarized in Table II. The measured gain, in the order of 21.7 dB, is remarkably stable with lens tilt and this behavior is extended up to 50° tilt; corresponding beam direction is near 45°, almost doubling the maximum scan angle of the L1 lens, considering the same 2 dB scan loss criteria. Furthermore, the lens ensures considerable low cross polarization level for all tilt angles and the radiation efficiency is above 95%.

CST simulations have shown that the L2 lens performance is also very stable across the entire WirelessHD frequency band, with only ± 1 dB gain variation (Fig. 14).

Additional simulations were performed to determine the possible improvement of adding a quarter wavelength matching layer at the bottom lens surface [23]. The resulting reduction of $|s_{11}|$ at the horn input port is noticeable only for near-zero lens tilts; $|s_{11}|$ lowers by 5 dB and gain improves by $+0.6$ dB. However, for increasing tilt angles, this minor improvement decreases and even reaches -0.4 dB gain reduction for 50° lens tilt. This effect is observed since the matching layer depth is constant, equal to $\lambda_d/4 = 0.969$ mm, and therefore it performs better for near to normal incidence, which is not the case for large lens tilts.

Simulations were performed also for the case where the matching layer was extended to the upper surface, completely

TABLE II
MEASURED PERFORMANCE INDICATOR VALUES OF THE L2 LENS AT 62.5 GHZ VERSUS LENS TILT α. $\alpha_{\rm beam}$ INDICATES THE MAIN BEAM DIRECTION, ΔG IS THE SCAN LOSS VALUE, XPOL IS THE HIGHER CROSS POLARIZATION LEVEL IN THE MAIN BEAM FULL WIDTH AT -10 dB AND η IS THE CST SIMULATED RADIATION EFFICIENCY

L2 Lens					
α	α_{beam}	G (dBi)	ΔG (dB)	XPol (dB)	η (%)
0º	0.0º	21.7	0.0	-17.3	95.3
10º	9.7º	21.7	0.0	-16.2	95.5
20º	19.5º	21.7	0.0	-16.5	95.4
30º	27.9º	21.7	0.0	-16.5	95.8
40º	36.4º	21.2	0.5	-16.4	96.0
50º	44.8º	20.6	1.1	-16.5	97.0

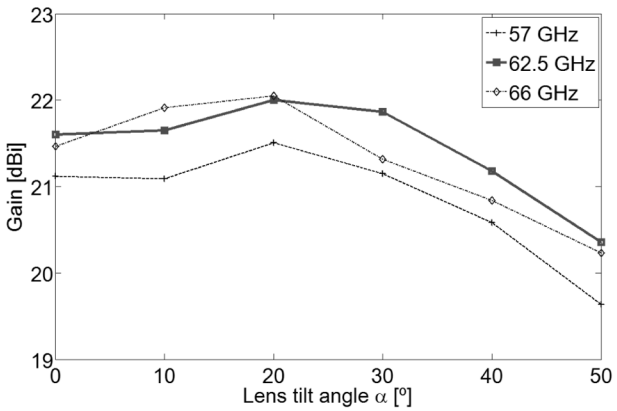

Fig. 14. Gain variation of the L2 lens versus tilt angle computed for three frequencies within the WirelessHD band.

surrounding the lens. In this case the improvement in gain is $+1.3$ dB for the non-tilted case, however it decreases with lens tilt down to -0.3 dB for 50° lens tilt.

In summary, although the matching layer improves the lens gain by more than 1 dB, the gain scan loss characteristic slightly degrades. But, above all, the additional manufacturing complexity of including a matching layer is not worth given the already excellent performance of the L2 lens without matching layer.

V. CONCLUSION

This paper introduced a simple, compact and low-cost antenna solution to perform total mechanical beam steering in the 60-GHz WirelessHD band, intended preferably for a fixed terminal like the flat TV screen. The beam steering is obtained by pivoting an appropriately shaped dielectric lens in front of a single fixed feed. The fabricated lens assembly demonstrated -45° to $+45^\circ$ elevation scan capability over full azimuth, with better than -1.1 dB gain scan loss and radiation efficiency always above 95%. Circular polarization is used to minimize polarization mismatch that can occur in line-of-sight links with linear polarization portable equipment, but the same concept was also tested with similar performance using linear polarization.

The polyethylene lens weights only 8 g; this is a favorable attribute for mechanical steering. The lens can be produced with insignificant cost using molding technique.

Higher beam tilt angles can be obtained by using higher permittivity materials. However, a carefully study is required to evaluate how the more intense reflections at the lens interfaces will deteriorated the overall lens performance and how the inclusion of matching layers can help in this case.

The presented antenna solution can be readily adjusted for other candidate application: the High Altitude Platform System (HAPS) application. In fact, changing the operating frequency is straight forward, involving almost only scaling of the complete solution. A different desired gain can be achieved just by changing the lens overall size.

ACKNOWLEDGMENT

The authors acknowledge the collaboration from V. Fred for prototype construction, and A. Almeida for prototype measurements.

REFERENCES

[1] R. Daniels and R. Heath, Jr, "60 GHz wireless communications: Emerging requirements and design recommendations," *IEEE Veh. Technol. Mag.*, vol. 2, no. 3, pp. 41–50, Sep. 2007.
[2] WirelessHD Specification Version 1.0 Overview, 2007 [Online]. Available: http://www.wirelesshd.org/
[3] C. Fernandes, "Shaped dielectric lenses for wireless millimeter-wave communications," *IEEE Antennas Propagat. Mag.*, vol. 41, no. 5, pp. 141–150, Oct. 1999.
[4] C. Fernandes and J. Fernandes, "Performance of lens antennas in wireless indoor millimeter-wave applications," *IEEE Trans. Microw. Theory Tech.*, vol. 47, no. 6, pt. 1, pp. 732–737, Jun. 1999.
[5] C. Fernandes, "Shaped-Beam Antennas," in *Handbook of Antennas in Wireless Communications*, L. Godara, Ed. New York: CRC Press, 2001, ch. 15.
[6] W. Menzel, D. Pilz, and M. A. Tikrit, "Millimeter- wave folded reflector antennas with high gain, low loss, and low profile," *IEEE Antennas Propagat. Mag.*, vol. 44, no. 3, pp. 24–29, Jun. 2002.
[7] V. Fusco, "Mechanical beam scanning reflect array," *IEEE Trans. Antennas Propagat.*, vol. 53, no. 11, pp. 3842–3844, Nov. 2005.
[8] K. Chang and M. L. T. Y. Rodenbeck, "Novel low-cost beam-steering techniques," *IEEE Trans. Antennas Propagat.*, vol. 50, no. 5, pp. 618–627, May 2002.
[9] K. V. Caekenberghe, T. Vaha-Heikkila, G. Rebeiz, and K. Sarabandi, "Ka-band MEMS TTD passive electronically scanned array (ESA)," in *Proc. IEEE APS/URSI Symp.*, Albuquerque, NM, Jul. 2006, pp. 513–516.
[10] A. Tombak and A. Mortazawi, "A novel low-cost beam-steering technique based on the extended-resonance power-dividing method," *IEEE Trans. Microw. Theory Tech.*, vol. 52, no. 2, pp. 664–669, Feb. 2004.
[11] B. Schoenlinner, X. Wu, J. Ebling, G. Eleftheriades, and G. Rebeiz, "Wide-scan spherical-lens antennas for automotive radars," *IEEE Trans. Microw. Theory Tech.*, vol. 50, no. 9, pp. 2166–2175, Sep. 2002.
[12] H. Kawahara, H. Deguchi, M. Tsuji, and H. Shigesawa, "Design of rotational dielectric dome with linear array feed for wide-angle multibeam antenna applications," *Electronics and Communications in Japan, Part 2*, vol. 90, no. 5, pp. 49–57, 2007.
[13] V. Manasson, L. Sadovnik, and R. Mino, "MMW scanning antenna," *IEEE Aerospace Electronic Syst. Mag.*, vol. 11, no. 10, pp. 29–33, Oct. 1996.
[14] A. Peebles, "A dielectric bifocal lens for multibeam antenna applications," *IEEE Trans. Antennas Propagat.*, vol. 36, no. 5, pp. 599–606, May 1988.
[15] D. Filipovic, S. Gearhart, and G. Rebeiz, "Double-slot antennas on extended hemispherical and elliptical silicon dielectric lenses," *IEEE Trans. Microw. Theory Tech.*, vol. 41, no. 10, pp. 1738–1749, Oct. 1993.
[16] J. Costa and C. Fernandes, "Broadband slot feed for integrated lens antennas," *IEEE Antennas Wireless Propagat. Lett.*, vol. 6, pp. 396–400, Sep. 2007.
[17] G. Godi, R. Sauleau, and D. Thouroude, "Performance of reduced size substrate lens antennas for millimetre-wave communications," *IEEE Trans. Antennas Propagat.*, vol. 53, no. 4, pp. 1278–1286, Apr. 2005.

[18] J. Costa, C. Fernandes, G. Godi, R. Sauleau, L. L. Coq, and H. Legay, "Compact Ka-band lens antennas for LEO satellites," *IEEE Trans. Antennas Propagat.*, vol. 56, no. 6, pp. 1251–1268, May 2008.
[19] Computer Simulation Technology, CST, 2008 [Online]. Available: http://www.cst.com/
[20] L. Chen, C. Ong, C. Neo, V. Varadan, and V. Varadan, *Microwave Electronics: Measurement and Materials Characterization*. London, U.K.: Wiley, 2004.
[21] E. Lima, J. Costa, M. Silveirinha, and C. Fernandes, "ILASH—Software tool for the design of integrated lens antennas," in *Proc. IEEE APS/URSI Symp.*, San Diego, CA, Jul. 2008.
[22] D. Pasqualini and S. Maci, "High-frequency analysis of integrated dielectric lens antennas," *IEEE Trans. Antennas Propagat.*, vol. 52, no. 3, pp. 840–847, Mar. 2004.
[23] M. van der Vorst, P. de Maagt, and M. Herben, "Effect of internal reflections on the radiation properties and input admittance of integrated lens antennas," *IEEE Trans. Microw. Theory Tech.*, vol. 47, no. 9, pp. 1696–1704, Sep. 1999.

Jorge R. Costa (S'97–M'03) was born in Lisbon, Portugal, in 1974. He received the Licenciado and Ph.D. degrees in electrical engineering from the Instituto Superior Técnico, Lisbon, Portugal, in 1997 and 2002, respectively.

He is currently a Researcher at the Instituto de Telecomunicações, Lisbon, Portugal. He is also an Assistant Professor at the Departamento de Ciências e Tecnologias da Informação, Instituto Superior de Ciências do Trabalho e da Empresa. His present research interests include lenses, reconfigurable antennas, MEMS switches, UWB and RFID antennas.

Eduardo B. Lima was born in Viseu, Portugal, in 1978. He received the Licenciado degree in electrical engineering from the Instituto Superior Técnico, Lisbon, Portugal, in 2003. He is a Researcher at the Instituto de Telecomunicações, Lisbon, Portugal, and he is currently working toward the M.Sc. degree in electrical engineering at the Instituto Superior Técnico.

From 2004 to 2007, he was involved on the ESA/ESTEC project ILASH (Integrated Lens Antenna Shaping). His present research interests include lenses and reflectors for focused systems.

Carlos A. Fernandes (S'86–M'89–SM'08) received the Licenciado, M.Sc., and Ph.D. degrees in electrical and computer engineering from Instituto Superior Técnico (IST), Technical University of Lisbon, Lisbon, Portugal, in 1980, 1985, and 1990, respectively.

He joined the IST in 1980, where he is presently a Full Professor in the Department of Electrical and Computer Engineering in the areas of microwaves, radio wave propagation and antennas. He is a Senior Researcher at the Instituto de Telecomunicações and coordinator of its Wireless Communications scientific area. He has been the leader of antenna activities in National and European Projects as RACE 2067—MBS (Mobile Broadband System), ACTS AC230—SAMBA (System for Advanced Mobile Broadband Applications) and ESA/ESTEC—ILASH (Integrated Lens Antenna Shaping). He has co-authored a book, a book chapter, and more than 100 technical papers in international journals and conference proceedings, in the areas of antennas and radiowave propagation modeling. His current research interests include dielectric antennas for millimeter wave applications, antennas and propagation modeling for personal communication systems, artificial dielectrics and metamaterials.